

1-, 3- and 8-substituted-9-deazaxanthines as potent and selective antagonists at the human A_{2B} adenosine receptor

Angela Stefanachi,^a Jose Manuel Brea,^c Maria Isabel Cadavid,^c Nuria B. Centeno,^d Cristina Esteve,^e Maria Isabel Loza,^c Ana Martinez,^b Rosa Nieto,^b Enrique Raviña,^b Ferran Sanz,^d Victor Segarra,^e Eddy Sotelo,^b Bernat Vidal^e and Angelo Carotti^{a,*}

^aDipartimento Farmaco-chimico, Università di Bari, via Orabona 4, I-70125 Bari, Italy

^bDepartamento de Química Orgánica, Universidade de Santiago de Compostela, E-15782 Santiago de Compostela, Spain

^cDepartamento de Farmacología, Universidade de Santiago de Compostela, E-15782 Santiago de Compostela, Spain

^dUnitat de Recerca en Informàtica Biomèdica (GRIB), IMIM-UPF, C/Dr. Aiguader 80, E-08003 Barcelona, Spain

^eAlmirall Research Center, Laboratorios Almirall S.A., Ctra. Laureà Miró 408, E-08980 St. Feliu de Llobregat, Barcelona, Spain

Received 7 September 2007; revised 20 December 2007; accepted 4 January 2008

Available online 10 January 2008

Abstract—A large series of piperazin-, piperidin- and tetrahydroisoquinolinamides of 4-(1,3-dialkyl-9-deazaxanthin-8-yl)phenoxyacetic acid were prepared through conventional or multiple parallel syntheses and evaluated for their binding affinity at the recombinant human adenosine receptors, chiefly at the hA_{2B} and hA_{2A} receptor subtypes. Several ligands endowed with high binding affinity at hA_{2B} receptors, excellent selectivity over hA_{2A} and hA_3 and a significant, but lower, selectivity over hA_1 were identified. Among them, piperazinamide derivatives **23** and **52**, and piperidinamide derivative **69** proved highly potent at hA_{2B} ($K_i = 11$, 2 and 5.5 nM, respectively) and selective towards hA_{2A} (hA_{2A}/hA_{2B} SI = 912, 159 and 630, respectively), hA_3 (hA_3/hA_{2B} SI = > 100, 3090 and >180, respectively) and hA_1 (hA_1/hA_{2B} SI = > 100, 44 and 120, respectively), SI being the selectivity index. A number of selected ligands tested in functional assays in vitro showed very interesting antagonist activities and efficacies at both A_{2A} and A_{2B} receptor subtypes, with pA_2 values close to the corresponding pK_i s. Structure–affinity and structure–selectivity relationships suggested that the binding potency at the hA_{2B} receptor may be increased by lipophilic substituents at the N4-position of piperazinamides and that an *ortho*-methoxy substituent at the 8-phenyl ring and alkyl groups at N1 larger than the ones at N3, in the 9-deazaxanthine ring, may strongly enhance the hA_{2A}/hA_{2B} SI.

© 2008 Elsevier Ltd. All rights reserved.

1. Introduction

Adenosine, a naturally occurring nucleoside, modulates several important physiological and pathological events by increasing the ratio of oxygen supply on demand, protecting against ischaemic injuries, triggering anti-inflammatory responses and promoting angiogenesis.^{1–3} Four diverse G-protein-coupled adenosine receptor (AdoR) subtypes— A_1 , A_{2A} , A_{2B} and A_3 —have been identified and characterized at the biological, pharmacological and physiological level.⁴ They differ in amino acid sequence, tissue distribution, effector coupling and

biological and pharmacological profiles. Among the four AdoR subtypes, A_{2B} receptor has been recently the object of an intense medicinal chemistry research since growing evidence indicated that its antagonists, and agonists as well, may have a variety of potential therapeutic applications.^{5,6} Indeed it has been shown that the activation of A_{2B} receptor subtypes may lead to: (i) an increase of intracellular calcium concentration and chloride ion secretion in intestinal cells (thus causing gastrointestinal irritations),⁷ (ii) an increased formation and release of a cerebral interleukin, IL-6, which has been associated with dementias and Alzheimer's disease (AD),⁸ (iii) an increased production of hepatic glucose,⁹ (iv) a stimulation of angiogenesis in endothelial cells,¹⁰ (v) an induction of apoptosis in arterial smooth muscle cells¹¹ and (vi) an over-stimulation of mast cells, thereby inducing hypersensitive disorders, hay fever and atopic eczema.^{12–16} Selective A_{2B} receptor antagonists may therefore play a role in important pathologies such

Keywords: 1,3-Dialkyl-6-substituted-1*H*-pyrrolo[3,2-*d*]pyrimidine-2,4(3*H*,5*H*)-diones; 9-Deazaxanthines; Adenosine receptor antagonists; hA_{2B} and hA_{2A} binding affinities; hA_{2A}/hA_{2B} selectivity; Structure–affinity relationships; Structure–selectivity relationships.

* Corresponding author. Tel.: +39 080 5442782; fax: +39 080 5442230; e-mail: carotti@farmchim.uniba.it

as gastrointestinal (i.e., diarrhoea),¹⁷ neurological (i.e., AD and dementia) and hypersensitive disorders (i.e., asthma), and in diabetes,⁹ atherosclerosis,¹⁸ restenosis¹⁸ and cancer.¹¹ Our main interest in this challenging scenario was the development of selective A_{2B} antagonists as potential antiasthmatic agents.

The rationale of our research was based on the observation that the bronchodilating activity of theophylline, and its structural analogue enprofylline, may be ascribed to a selective, albeit small, antagonism at the A_{2B} AdoRs.¹⁹ These findings prompted several groups to design and test a large number of xanthine derivatives in the search for new, more potent and A_{2B}-selective ligands.^{20–24} Indeed, besides the low active and A_{2B} selective **1** and **2**, in the last few years very potent and highly A_{2B}-selective xanthines,^{25–29} such as XAC (**3**),³⁰ MRS1754 (**4**),³¹ **5**,³¹ **8**,³² **9**,³³ **10**,³⁴ and 9-dAXs such as **6** and **7**³⁵ (Chart 1), have been discovered.

Since 9-deazaxanthines (9-dAXs) have been only rarely studied, especially for their antagonistic activity at the A_{2B}receptor,^{22,24} we began a systematic study addressing first an easy, efficient and expeditious synthetic pathway to fully functionalized 9-dAXs followed by a thorough investigation of their biological and pharmacological properties.³⁵ Our goal was to discover potent ($K_i < 50$ nM) antagonists of human A_{2B} receptor (hA_{2B}) with at least 100-fold selectivity over hA_{2A} and, possibly, over the other two AdoR subtypes, namely hA_1 and hA_3 . A first account of this study dealing more specifically with the synthesis, biological and pharmaco-

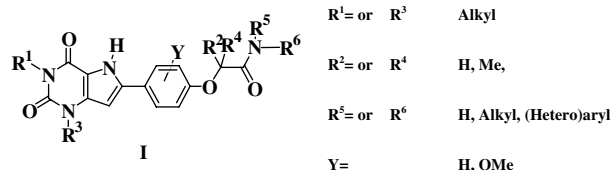


Chart 2. General structure and main structural variations of 9-dAX AdoR ligands.

logical evaluation of 9-dAX derivatives bearing a phenyl or benzyl oxyacetamido group on the *para* position of the 8-phenyl ring (see general structure **I** in Chart 2) has been recently published.³⁵ Our investigation led to the discovery of ligands endowed with sub-micromolar to low nanomolar binding affinity at hA_{2B} receptors, good selectivity over hA_{2A} and hA_3 and a relatively poor selectivity over hA_1 . Good antagonistic potencies and efficacies, with pA_2 values close to the corresponding pK_i s, were observed in functional in vitro assays performed on a selected series of compounds.³⁵ *para*-Bromoanilides of 4-(1,3-dimethyl-9-deazaxanthin-8-yl) phenoxyacetic acid proved to be the most interesting leads, showing outstanding hA_{2B} affinity ($pK_i = 8.58$ and 8.46 , respectively) and a high selectivity index ($SI = K_i hA_x / K_i hA_{2B}$) over hA_{2A} , hA_3 and hA_1 ($741 > 1000$, 11.7 and 1412 , 3090 , 9.3 for compounds **6** and **7**, respectively, in Chart 1).

As a continuation of our ongoing research in the field we designed, synthesized and evaluated at AdoRs a new series of 9-dAXs, which differs from previously reported

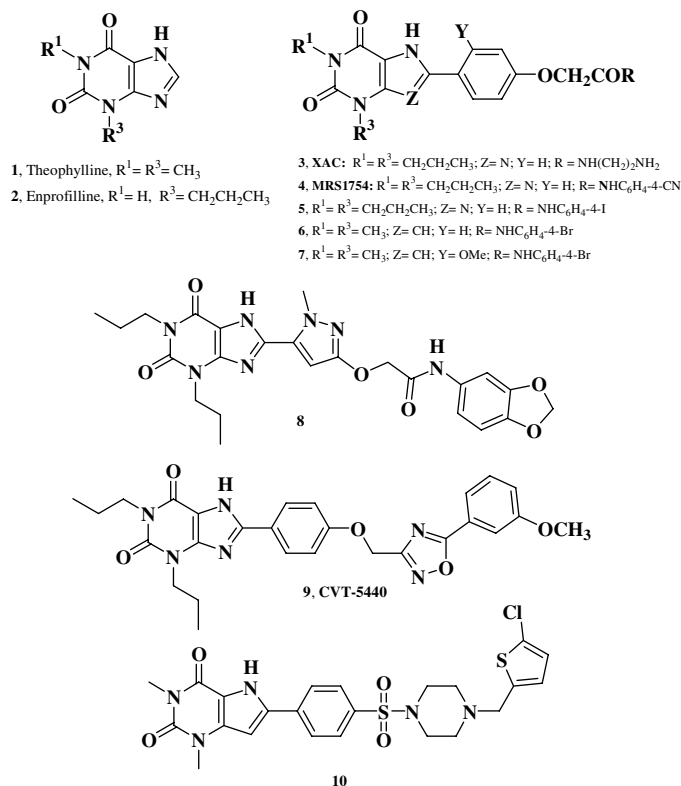
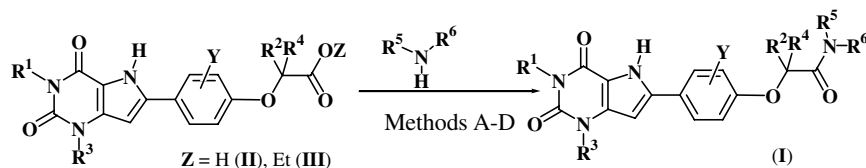


Chart 1. Xanthines and 9-dAX derivatives with antiasthmatic (**1** and **2**) and selective A_{2B} AdoR antagonistic activities (**3–10**).



Scheme 1. Reagents: method A (Z = Et): NaCN/dioxane, reflux/sealed tube. Method B (Z = H): isobutyl chloroformate/NMM/THF. Method C (Z = H): EDC/OHBT/triethylamine. Method D (Z = H): EDC/OHBT/polymer bound morpholine.

ligands mainly in the NR^5R^6 moieties, which now consist of heterocyclic amines (i.e., piperazines, piperidines and tetrahydroisoquinolines).

2. Chemistry

The synthesis of 9-dAX (1,3-dialkyl-8-substituted-1*H*-pyrrrolo[3,2-*d*]pyrimidine-2,4(3*H*,5*H*)-diones) acid and ester intermediates (**II** and **III**) was performed according to our previously published procedures.³⁵ The synthetic strategies (see Scheme 1) to obtain cyclic amides **I**, reported in Tables 1–3, include the use of conventional syntheses (methods A–C) as well as a procedure adapted to medium-throughput parallel synthesis (method D).

The first amidation procedure (Scheme 1, method A) implies the reaction of the 9-dAX esters with an excess of the appropriate amine and a catalytic amount of sodium cyanide in dioxane at reflux or under appropriate heating in a sealed tube. In a second procedure (method B), the carboxylic acids were converted into mixed anhydride intermediates, by treatment with isobutyl chloroformate and *N*-methylmorpholine (NMM), and then reacted with the proper amines. The other amidation methods involved direct condensation of carboxylic acids and the suitable amines in polar aprotic solvents (DMF, tetrahydrofuran) in the presence of an organic base (triethylamine or polymer supported morpholine) and 1-[3-dimethylaminopropyl]-3-ethylcarbodiimide hydrochloride (EDC) and 1-hydroxybenzotriazole (OHBT) (methods C and D) as coupling reagents. Molecules with chiral centres were isolated and tested as racemic mixtures.

3. Biochemical and pharmacological assays

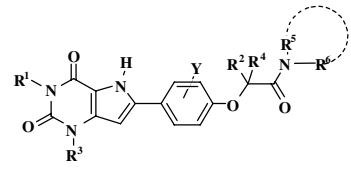
Compounds were assayed for their ability to displace [³H]DPCPX, [³H]ZM241385, [³H]DPCPX and [³H]NECA from cloned human A_1 , A_{2A} , A_{2B} and A_3 AdoRs. All the active compounds showed competition concentration–response curves of specific radioligand binding against increasing concentrations of ligands, the slopes not being significantly different from unity at the 5% level of statistical significance. A representative binding competition curve is shown in Figure 1a for ligand **17**. Antagonistic activity and efficacy were measured for a few selected ligands by means of isolated organs assay at both guinea pig A_{2B} and rat A_{2A} AdoR subtypes. All the tested compounds concentration-dependently displaced the curves of the NECA AdoR

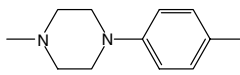
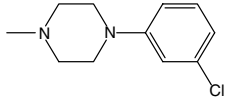
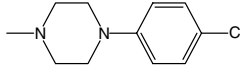
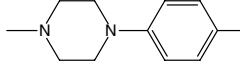
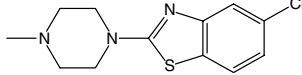
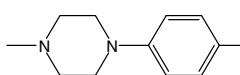
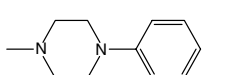
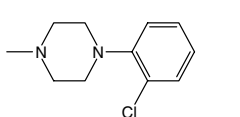
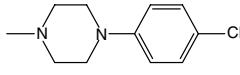
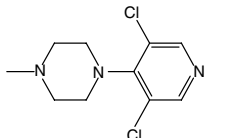
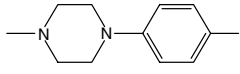
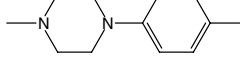
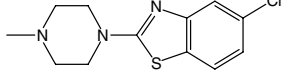
agonist to the right in a parallel way without depression of their maximum, which is the typical behavior of competitive antagonists. A representative example (ligand **17**) is shown in Figure 1b. The antagonist activity and efficacy of the tested ligands are collected in Table 4. Furthermore, antagonistic activity and efficacy at hA_{2A} and hA_{2B} receptors were measured for some selected ligands by means of cAMP assays on HEK-293 cells, endogenously over expressing hA_{2B} receptors, and over CHO cells transfected with hA_{2A} receptors. All the tested compounds concentration-dependently displaced the curves of the NECA AdoR agonist to the right in a parallel way without depression of their maximum, which is the typical behavior of competitive antagonists. A representative example (ligand **17**) is shown in Figure 1c.

4. Results and discussion

The chemical structures of all the examined novel ligands are reported in Tables 1–3 along with their binding affinities at the indicated AdoR subtype. It must be remembered that the main goal of our research is the discovery of new, highly active hA_{2B} antagonists endowed with a good hA_{2A}/hA_{2B} selectivity index and therefore only when ligands with these characteristics were identified the affinities for the other two AdoR subtypes, hA_1 and hA_3 , were measured. According to this strategy, the biological assays were performed up to the determination of the K_i only for those ligands found most promising in the initial biological screening. As a consequence, binding affinities at the hA_{2B} and hA_{2A} AdoR were firstly measured as a percentage of radioligand displacement at 0.1 (or 1) μM concentration and only when indicative of a high hA_{2B} AdoR affinity and likely high hA_{2A}/hA_{2B} SI; the K_i s were determined at both AdoR subtypes. For this reason, only the percentage of radioligand displacement at the indicated concentrations is reported for a few ligands in Tables 1–3.

For sake of clarity, the discussion of the structure–affinity (SAFIR) and structure–selectivity relationships (SSR) is given here separately for each class of ligands, according to the structural classification reported in Tables 1–3, where examined ligands are ordered within structural types on the basis of their decreasing hA_{2B} affinity expressed as $\text{p}K_i$ s. The percentage of radioligand displacement at 0.1 or 1 μM is reported for low active compounds or compounds whose low solubility prevented the determination of their K_i . Selectivity is referred to the hA_{2B} AdoR and is expressed as selectivity

Table 1. Chemical structures and binding affinities^a at the hA_{2B} AdoR of 1,3-dialkyl-9-dAX piperazinamides **11–66**


Compound	R ¹ /R ³	R ² /R ⁴	NR ⁵ R ⁶	Y	pK _i /hA _{2B}	pK _i /hA _{2A}	hA _{2A} /hA _{2B} SI	pK _i A ₁	pK _i A ₃
11	CH ₃ /CH ₃	CH ₃ /H		H	8.74	6.41	213	nd	nd
12	CH ₃ /CH ₃	H/H		H	8.55	6.81	55	nd	nd
13	CH ₃ /CH ₃	H/H		H	8.47	6.40	117	nd	nd
14	CH ₃ /CH ₃	H/H		H	8.46	6.94	33.1	nd	nd
15	CH ₃ /CH ₃	H/H		H	8.44	6.74	50.1	nd	nd
16	CH ₃ /CH ₃	H/H		H	8.38	6.88	31.6	nd	nd
17	CH ₃ /CH ₃	H/H		H	8.28	6.97	20.4	6.30	20% at 1 μM
18	CH ₃ /CH ₃	H/H		H	8.20	6.45	56	nd	nd
19	CH ₃ /CH ₃	H/H		H	8.20	6.45	56	nd	nd
20	CH ₃ /CH ₃	H/H		H	8.15	21% at 1 μM	nd	nd	nd
21	CH ₃ /CH ₃	CH ₃ /H		H	8.09	6.57	26	nd	nd
22	CH ₃ /CH ₃	H/H		H	8.02	6.49	33.8	nd	nd
23	CH ₃ /CH ₃	CH ₃ /CH ₃		H	7.96	5.00	912	8% at 1 μM	18% at 1 μM

(continued on next page)

Table 1 (continued)

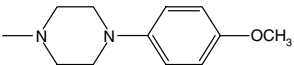
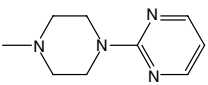
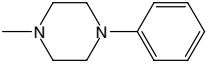
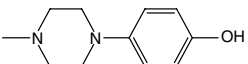
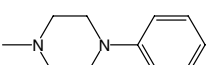
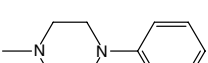
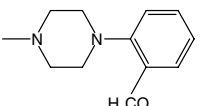
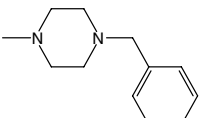
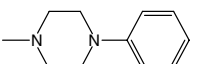
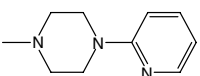
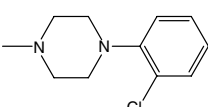
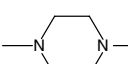
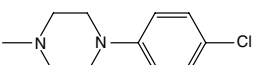
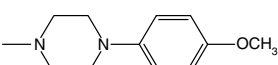
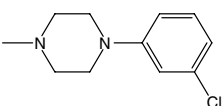
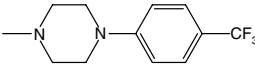
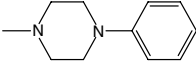
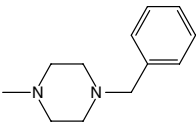
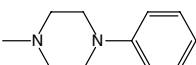
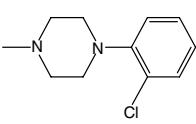
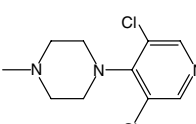
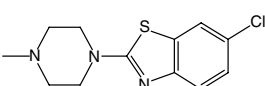
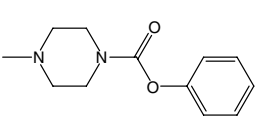
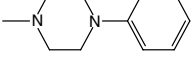
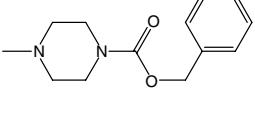
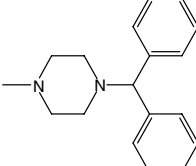
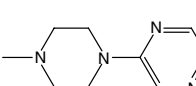
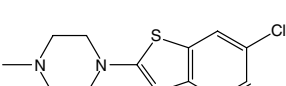
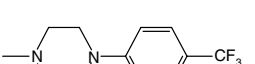
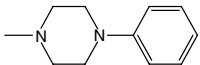
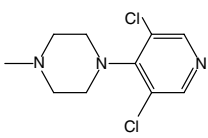
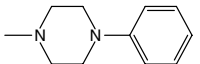
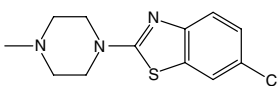
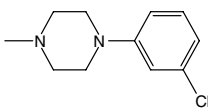
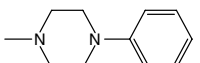
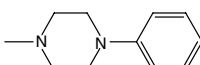
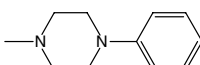
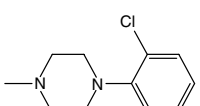
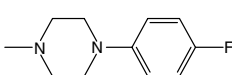
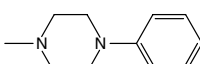
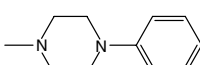
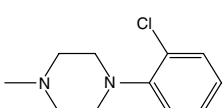
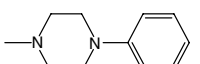
Compound	R ¹ /R ³	R ² /R ⁴	NR ⁵ R ⁶	Y	p <i>K</i> _i hA _{2B}	p <i>K</i> _i hA _{2A}	hA _{2A} /hA _{2B} SI	p <i>K</i> _i A ₁	p <i>K</i> _i A ₃
24	CH ₃ /CH ₃	H/H		H	7.88	6.77	12.9	nd	nd
25	CH ₃ /CH ₃	H/H		H	7.87	6.38	30.9	nd	nd
26	CH ₃ /CH ₃	CH ₃ /H		H	7.69	6.45	17.4	nd	nd
27	CH ₃ /CH ₃	H/H		H	7.56	6.21	22	nd	nd
28	CH ₃ /CH ₃	CH ₃ /CH ₃		H	7.50	6.76	5.49	nd	nd
29	CH ₃ /CH ₃	H/H		<i>o</i> -OCH ₃	7.49	5.15	218.8	6.27	9% at 1 μM
30	CH ₃ /CH ₃	H/H		H	7.29	5.63	45.7	nd	n.d
31	CH ₃ /CH ₃	H/H		H	7.27	5.81	28.8	nd	nd
32	CH ₃ /CH ₃	H/H		<i>m</i> -OCH ₃	7.24	5.84	25.1	nd	nd
33	CH ₃ /CH ₃	H/H		H	7.23	6.15	12	nd	nd
34	CH ₃ /CH ₃	CH ₃ /H		H	7.15	6.13	10.5	nd	nd
35	CH ₃ /CH ₃	H/H		H	6.76	6.10	4.05	nd	nd
36	CH ₃ /CH ₃	H/H		<i>o</i> -OCH ₃	6.32	4% at 1 μM	—	nd	nd
37	CH ₃ /CH ₃	H/H		<i>o</i> -OCH ₃	30% at 0.1 μM	1% at 0.1 μM	—	nd	nd
38	Pr/Pr	H/H		H	8.82	6.94	75.9	nd	nd

Table 1 (continued)

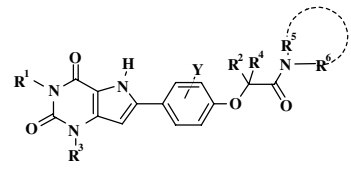
Compound	R ¹ /R ³	R ² /R ⁴	NR ⁵ R ⁶	Y	pK _i /hA _{2B}	pK _i /hA _{2A}	hA _{2A} / hA _{2B} SI	pK _i A ₁	pK _i A ₃
39	Pr/Pr	H/H		H	8.38	6.76	41.7	nd	nd
40	Pr/Pr	H/H		H	8.32	6.79	33.8	nd	nd
41	Pr/Pr	H/H		H	8.21	6.59	41.7	nd	nd
42	Pr/Pr	CH ₃ /H		H	8.18	6.62	36.3	nd	nd
43	Pr/Pr	H/H		H	8.16	7.42	5.5	nd	nd
44	Pr/Pr	H/H		H	8.12	7.13	9.8	nd	nd
45	Pr/Pr ₂	H/H		H	7.98	6.09	77.6	nd	nd
46	Pr/Pr	H/H		H	7.69	6.81	7.6	nd	nd
47	Pr/Pr	CH ₃ /CH ₃		H	7.61	6.58	10.7	nd	nd
48	Pr/Pr	H/H		H	7.41	6.82	3.9	nd	nd
49	Pr/Pr	H/H		H	7.29	5.8	30.9	nd	nd
50	Pr/Pr	H/H		H	7.00	11% at 0.1 μM	nd	nd	nd
51	CH ₃ /Pr	CH ₃ /CH ₃		H	8.98	9% at 1 μM	nd	nd	nd
52	CH ₃ /Pr	H/H		H	8.69	6.49	158.5	7.05	5.65

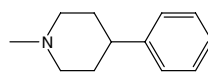
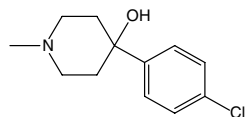
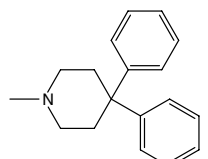
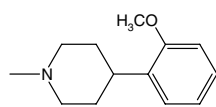
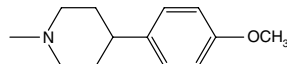
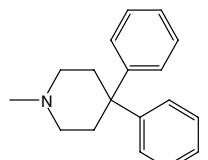
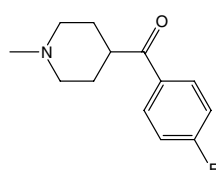
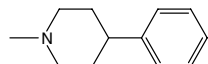
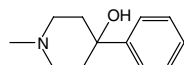
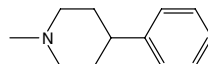
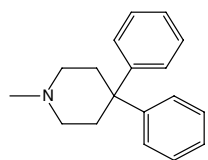
(continued on next page)

Table 1 (continued)

Compound	R ¹ /R ³	R ² /R ⁴	NR ⁵ R ⁶	Y	pK _i /hA _{2B}	pK _i /hA _{2A}	hA _{2A} /hA _{2B} SI	pK _i A ₁	pK _i A ₃
53	CH ₃ /Pr	CH ₃ /CH ₃		H	8.38	6.25	134.9	nd	nd
54	CH ₃ /Pr	H/H		H	8.37	6.19	151.4	nd	nd
55	CH ₃ OCH ₂ CH ₂ /CH ₃ OCH ₂ CH ₂	H/H		H	8.31	6.40	81	nd	nd
56	CH ₃ /Pr	H/H		H	8.24	6.20	106	nd	nd
57	CH ₃ /Pr	H/H		H	8.22	6.32	79	nd	nd
58	(CH ₃) ₂ CH CH ₂ /Pr	H/H		H	8.13	15% at 1 μM	nd	nd	nd
59	Cypropyl- CH ₂ /cypro- pyl-CH ₂	H/H		H	7.93	7.31	4.2	nd	nd
60	Pr/CH ₃	H/H		H	7.88	6.50	24	nd	nd
61	CH ₃ /Pr	H/H		H	7.83	5.96	74.1	nd	nd
62	CH ₃ /Pr	H/H		H	7.82	6.33	30.9	nd	nd
63	CH ₃ CH ₂ / CH ₃ CH ₂	H/H		H	7.59	6.16	26.9	nd	nd
64	CH ₃ /Pr	H/H		H	7.59	6.15	27.5	nd	nd
65	Pr/CH ₃	H/H		H	7.16	6.65	3.2	nd	nd
66	CF ₃ CH ₂ / CF ₃ CH ₂	H/H		H	32% at 0.1 μM	3% at 0.1 μM	nd	nd	nd

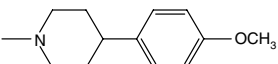
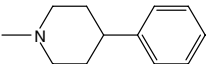
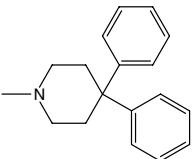
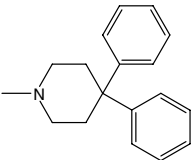
^a Affinity values are expressed as pK_i or as % of inhibition at the indicated concentration, SEMs were always lower than 10%.

Table 2. Chemical structures and binding affinities^a at the *hA*_{2B} AdoR of 1,3-dialkyl-9-dAX piperidinamides **67–81**


Compound	R ¹ /R ³	R ² /R ⁴	NR ⁵ R ⁶	Y	p <i>K</i> _i / <i>hA</i> _{2B}	p <i>K</i> _i / <i>hA</i> _{2A}	<i>hA</i> _{2A} / <i>hA</i> _{2B} SI	p <i>K</i> _i A ₁	p <i>K</i> _i A ₃
67	CH ₃ / <i>Pr</i>	H/H		H	8.59	5.99	398	nd	nd
68	CH ₃ /CH ₃	H/H		H	8.54	6.49	112.2	nd	nd
69	CH ₃ / <i>Pr</i>	H/H		H	8.25	5.45	630	6.17	4% at 1 μM
70	CH ₃ / <i>Pr</i>	H/H		H	8.21	6.39	66.1	nd	nd
71	CH ₃ / <i>Pr</i>	H/H		H	8.04	6.4	43.7	nd	nd
72	CH ₃ /CH ₃	H/H		H	8.02	28% at 1 μM	nd	nd	nd
73	CH ₃ /CH ₃	H/H		H	7.95	6.52	26.9	nd	nd
74	CH ₃ /CH ₃	H/H		H	7.91	6.10	64.6	nd	nd
75	<i>Pr</i> / <i>Pr</i>	H/H		H	7.87	5.94	85.1	nd	nd
76	<i>Pr</i> / <i>Pr</i>	H/H		H	7.68	6.23	28.2	nd	nd
77	<i>Pr</i> / <i>Pr</i>	H/H		H	7.67	5.98	40.7	nd	nd

(continued on next page)

Table 2 (continued)

Compound	R ¹ /R ³	R ² /R ⁴	NR ⁵ R ⁶	Y	p <i>K</i> _i <i>hA</i> _{2B}	p <i>K</i> _i <i>hA</i> _{2A}	<i>hA</i> _{2A} / <i>hA</i> _{2B} SI	p <i>K</i> _i A ₁	p <i>K</i> _i A ₃
78	CH ₃ /CH ₃	H/H		<i>m</i> -OCH ₃	7.51	6.06	28.18	nd	nd
79	CH ₃ /CH ₃	H/H		<i>o</i> -OCH ₃	6.05	3% at 1 μM	—	nd	nd
80	CH ₃ / <i>Pr</i>	CH ₃ /CH ₃		H	35% at 0.1 μM	11% at 0.1 μM	nd	nd	nd
81	CH ₃ /CH ₃	CH ₃ /CH ₃		H	34% at 0.1 μM	8% at 0.1 μM	nd	nd	nd

^a Affinity values are expressed as p*K*_i or as % of inhibition at the indicated concentration, SEMs were always lower than 10%.

index (SI), that is, the affinity ratio $K_i/hA_x/K_i/hA_{2B}$. For a more immediate and efficient analysis of the variation of both affinity and selectivity, the binding data are presented graphically as a plot of p*K*_i*hA*_{2A} (*Y*-axis) versus p*K*_i *hA*_{2B} (*X*-axis) using the same scale and range for both axes (square plot). Thus, on the diagonal of this plot ($Y = X$) lie compounds with equal affinities at both receptors, whereas highly *hA*_{2B} selective compounds will be seen far below the diagonal. The distance of their p*K*_i values from the diagonal is a direct measure of the degree of selectivity. Ligands targeted in the present work—those endowed with both high *hA*_{2B} affinity and high *hA*_{2A}/*hA*_{2B} SI—will be therefore located in the lower right-hand corner of the plots. Whenever possible, a comparative analysis was conducted among similarly substituted ligands belonging to different classes.

4.1. 1,3-Dialkyl-8-[4-phenoxy(*N*1-piperazinyl)acetamido]-9-deazaxanthines

A large array of 1,3-dialkyl-8-substituted-9-dAXs containing a piperazinyl NR⁵R⁶ group was prepared and evaluated for their binding affinity at *hA*_{2B} and *hA*_{2A} AdoRs (Table 1). Three different subclasses, constituted by 1,3-dimethyl (diM, 27 members), 1,3-dipropyl (diP, 13 members) and 1,3-dialkyl (diA, 16 members, containing different alkyl groups at positions 1 and 3) derivatives, are listed separately in Table 1 for a better evaluation of the SAFIRs and SSRs.

p*K*_i values ranging from 5.00 to 7.42 and from 6.32 to 8.98 were measured for *hA*_{2A} and *hA*_{2B} AdoR affinities, respectively. Their distribution and relationship can be seen in the colour square plot of p*K*_i*hA*_{2B} versus p*K*_i *hA*_{2A} of Figure 2 where diM, diP and diA derivatives are indicated in blue, pink and yellow, respectively. A simple visual inspection of the plot revealed that *hA*_{2B} and *hA*_{2A} binding affinities are not correlated and that

a number of examined ligands (lower right corner of the plot) were potent and strongly selective *hA*_{2B} receptor ligands. Indeed, both high p*K*_is (>7.45) and *hA*_{2A}/*hA*_{2B} SI > 50 were observed for many diM (i.e., **11–13**, **15**, **18**, **19**, **23** and **29**), diA (i.e., **51–57** and **61**) and two diP derivatives (i.e., **38** and **45**). The highest *hA*_{2A}/*hA*_{2B} SIs were shown by diM piperazinamide derivatives **11**, **29** and **23** (SI = 213, 219 and 912, respectively). The two most selective ligands **29** and **23** were tested also at the *hA*₁ and *hA*₃ AdoRs. Unfortunately, the low solubility of compound **23** prevented the determination of its *K*_i at both AdoRs. Nonetheless, the percentage of its radioligand displacement at *hA*₁ and *hA*₃ AdoRs (8% and 18%, respectively, at 1 μM) surely indicated high *hA*₁/*hA*_{2B} and *hA*₃/*hA*_{2B} SIs. Affinity data of **29** at *hA*₁ (p*K*_i = 6.27) and *hA*₃ (9% displacement at 1 μM) pointed out a low *hA*₁/*hA*_{2B} SI (SI = 17) and a presumed much higher *hA*₃/*hA*_{2B} SI, in full agreement with our previous findings.³⁵ The introduction of an *ortho*-methoxy group in the 8-phenyl ring of different ligands gave contrasting results. For lead compound **17** the *hA*₁/*hA*_{2B} SI increased by one order of magnitude (from 20.4 to 219 in compound **29**), as a result of a much stronger decrease of *hA*_{2A} than *hA*_{2B} affinity (p*K*_i from 6.97 to 5.15 and from 8.28 to 7.49, respectively). The same structural modification, that recently drove us to the identification of compound **7** (Chart 1), one of the most potent and *hA*_{2B}-selective antagonists discovered so far, resulted instead in a dramatic decrease of both *hA*_{2B} and *hA*_{2A} affinities for the *N*4-*para*-methoxyphenyl- and *N*4-*para*-chlorophenyl-piperazinamides (**24** vs **37** and **13** vs **36**). This unexpectedly high diminution of *hA*_{2B} affinity may be due to negative steric effects at the *para* position of the phenyl ring that may occur only when the phenyl ring at position 8 likely assumes a different conformation because of the presence of the *ortho*-methoxy group. Indeed, a conformational analysis indicated for the most stable conformers of the phenyl and *ortho*-

Table 3. Chemical structures and binding affinities^a at the *hA*_{2B} AdoR of 1,3-dialkyl-9-dAX tetrahydroisoquinolinamides **82–90**

Compound	R ¹ /R ³	R ² /R ⁴	NR ⁵ R ⁶	Y	p <i>K</i> _i <i>hA</i> _{2B}	p <i>K</i> _i <i>hA</i> _{2A}	<i>hA</i> _{2A} / <i>hA</i> _{2B} SI	p <i>K</i> _i A ₁	p <i>K</i> _i A ₃
82	<i>Pr/Pr</i>	H/H		H	8.64	7.03	40.7	nd	nd
83	<i>Pr/Pr</i>	CH ₃ /H		H	8.33	6.8	33.9	nd	nd
84	CH ₃ / <i>Pr</i>	H/H		H	8.14	6.00	138	nd	nd
85	CH ₃ /CH ₃	H/H		H	8.06	6.37	49	6.44	15% at 1 μM
86	Cypropyl-CH ₂ / cypropyl-CH ₂	H/H		H	8.02	6.62	25	nd	nd
87	CH ₃ / <i>Pr</i>	H/H		H	7.84	6.68	14.5	nd	nd
88	CH ₃ OCH ₂ CH ₂ / CH ₃ OCH ₂ CH ₂	H/H		H	7.77	20% at 1 μM	nd	nd	nd
89	CH ₃ /CH ₃	H/H		<i>o</i> -OCH ₃	7.36	4.92	275.4	6.57	15% at 1 μM
90	CH ₃ /CH ₃	H/H		<i>m</i> -OCH ₃	6.77	5.17	39	nd	nd

^a Affinity values are expressed as p*K*_i or as % of inhibition at the indicated concentration, SEMs were always lower than 10%.

methoxy phenyl congeners diverse N7C8C1'C2'(OMe) dihedral angles (nearly 30° and 0°, respectively). Very interestingly, the highly *hA*_{2B} selective ligand **11** was endowed also with an outstanding *hA*_{2B} affinity (*K*_i = 2 nM).

diM congeners generally showed *hA*_{2A}/*hA*_{2B} SIs close to those of the corresponding diP congeners (**12** versus **38**; **17** versus **40**; **16** versus **39** and **28** versus **47**), whereas 1-propyl-3-methyl derivatives displayed SIs higher than the corresponding diP/diM derivatives (**52** vs **39/16**; **53**

vs **47/28**; **54** vs **44**; **56** vs **45/15** and **61** vs **43/18**). The same observation holds for the 1-isobutyl-3-methyl derivative **58** which is much more selective than the corresponding diM derivative **17** (*hA*_{2A}/*hA*_{2B} SI > 400 vs 20). These results are consistent with literature data indicating higher *hA*_{2A}/*hA*_{2B} SIs for xanthines bearing alkyl substituents at position 1 larger than those at position 3.²¹ Notably, several highly *hA*_{2B} selective ligands (i.e., compounds **15**, **23**, **45**, **51** and **56**) presented a 5-chloro-2-benzothiazolyl substituent at the N4 position of the piperazine ring which may be likely engaged in

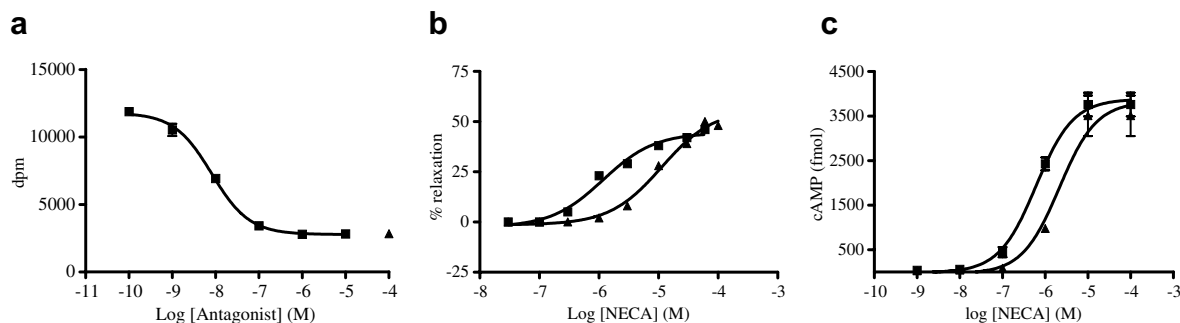


Figure 1. (a) Binding competition experiments at cloned hA_{2B} AdoR of compound **17** (■). Non-specific binding was measured with 10^{-3} M NECA (▲). The assay was performed in duplicate. (b) Functional assay with compound **17** at A_{2B} receptors in smooth muscle of guinea pig thoracic aorta. Cumulative concentration–response curves to NECA in the absence (■) and in the presence (▲) of **17**, 0.1 μ M. (c) Functional assay with compound **17** at hA_{2B} receptors expressed in HEK-293 cells. Cumulative concentration–response curves to NECA in the absence (■) and in the presence (▲) of **17**, 30 nM.

Table 4. Binding affinities and antagonist potency at A_{2B} and A_{2A} AdoRs of selected 9-dAXs^a

Compound	pK_i/hA_{2B}	pK_i/hA_{2A}	$pA_{2A}A_{2B}^b$	$pA_{2A}A_{2A}^c$
17	8.28	6.97	8.00	6.80
47	7.61	6.58	7.50	6.40
62	7.82	6.33	7.90	6.63
69	8.25	5.45	8.00	5.10
85	8.06	6.37	7.89	6.30

^a pK_i and pA_2 values represent means of at least three independent experiments with a SEM always lower than 10%.

^b Smooth muscle of guinea pig thoracic aorta.

^c Smooth muscle of male Sprague–Dawley rat aorta.

selective binding interactions with hA_{2A} and hA_{2B} binding sites. The effect of C-methylation at the alpha position of the oxyacetamido bridge on hA_{2B} AdoR affinity and selectivity was investigated with the synthesis and biological evaluation of a small series of mono- and dimethyl derivatives. While for most mono-C-methyl derivatives hA_{2A}/hA_{2B} SIs remained close to those of the starting methylene congeners (**14** vs **21**, **17** vs **26**, **40** vs **42**) a dramatic increase of SI (from 50 to 912) resulted from the C-dimethylation of the N4-chlorobenzothiazolyl derivative **15**. Compound **23** was in-

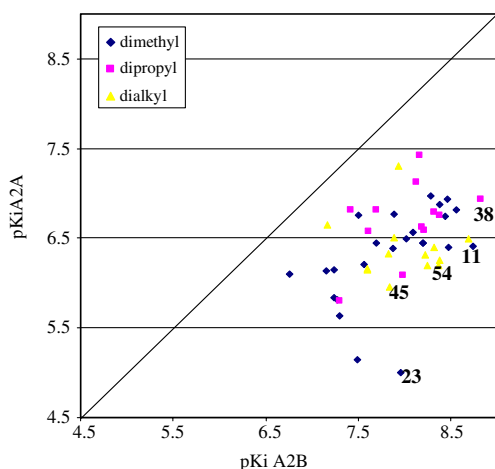


Figure 2. Affinity–selectivity plot for 1,3-dipropyl-9-dAX piperazinamides **11–66** (see Table 1).

deed the most hA_{2B} -selective ligand obtained in this work. In other cases an opposite effect resulted from C-dimethylation: compounds **28** and **47** showed SI values of 5 and 11, respectively, which were much lower than those observed for the corresponding monomethyl (**26** and **42**, respectively) and non-methylated congeners (**17** and **40**, respectively).

Other interesting insights can be inferred from the SAFIR study of piperazinamides in Table 1 that was limited to the hA_{2B} affinity since affinity data at hA_{2A} presented a much lower variance. As observed previously in anilide and benzamide series (Chart 2, structure **1**, $R_5 = H$, $R_6 = Ph$ or Bn), lipophilicity of the NR^5R^6 fragment plays a crucial role in the hA_{2B} -receptor binding as demonstrated by the higher affinity observed moving from the N4-methyl (**35**) to the -phenyl (**17**) and -benzyl (**31**) piperazine derivatives. The key role of lipophilicity of the N4-substituent was confirmed also by the lower hA_{2B} affinities found for the more hydrophilic 2-pyrimidinyl (**25**) and 2-pyridyl (**33**) diM derivatives and the 2-pyridazinyl diP derivative (**50**) compared to the corresponding N4-phenyl leads **17** and **40**, respectively. It is worth to note that heterocyclic rings substituted with lipophilic chloro substituents recovered a good hA_{2B} binding affinity (see the dichloropyridyl derivatives **20** and **44**). The introduction of one or two methyl groups on the oxyacetamido bridge led to a diminution of hA_{2B} affinity in both the diM and diP series, being the gem-dimethyl derivatives always less active than the corresponding monomethyl congeners, as resulted from the following rank of hA_{2B} affinity: **14** > **21**; **17** > **26** > **28**; **40** > **42** > **47**; **18** > **34**. The decreased hA_{2B} affinity of carbamate (**46** and **48**) and benzoyl (**49**) diP derivatives compared to the N4-phenyl lead **40** may be ascribed to negative steric effects. The SAFIR at hA_{2B} was assessed more thoroughly by introducing several substituents on the *ortho*, *meta* and *para* positions of the N4-phenyl ring of diM, diP and 1-propyl-3-methyl lead compounds **17**, **40** and **64**, respectively. The most explored class was that of diM congeners. Substituents at the phenyl ring were chosen to properly sample the physicochemical domain of their steric, lipophilic and electronic properties. Once again, the substituent lipophilicity was a crucial determinant

of a high hA_{2B} affinity. Compounds bearing lipophilic substituents in *meta* and *para* positions were more active than lead compounds in all the three series (i.e., **12–14**, **16** > **17**; **38**, **39** > **40** and **52**, **57**, **61**, **62** > **64**). It is worth noting that the lipophilic effect depends on the substituent position on the phenyl ring: *meta*-chloro derivatives were found to be highly potent in all three series, whereas *ortho*-chloro derivatives **18** and **34** proved less active than lead compound **17**, most likely for a negative steric effect at the *ortho* position. The same consideration hold for the *ortho*-methoxy derivative **30** which showed an affinity much lower than both the corresponding *para*-congener **24** and lead compound **17**. The introduction of hydrophilic *para*-substituents such as methoxy, hydroxyl and cyano produced a decrease of hA_{2B} affinity (lead compound **17** vs **19**, **24** and **27**, respectively); this lent support to the hypothesis that favourable lipophilic interactions took place at the N4 region of the piperazine ring and in particular, in the accessible regions around the N4-phenyl ring. A further proof to this hypothesis came from the observation that in the diM and diP series the highest hA_{2B} affinity was displayed by the highly lipophilic 3-chlorophenyl derivatives **12** and **38** ($K_i = 3$ and 1.5 nM, respectively) whereas in the diA series the chorobenzothiazolyl derivative **51** yielded the most potent hA_{2B} AdoR ligand found in the present work ($K_i = 1$ nM).

4.2. 1,3-Dialkyl-8-[4-phenoxy(*N*-piperidinyl)acetamido]-9-deazaxanthines

Fifteen 1,3-dialkyl-9-dAX derivatives bearing a 4-substituted piperidine as the NR^5R^6 moiety (structure **I**, Chart 2) were prepared and evaluated for their affinity at hA_{2B} and hA_{2A} AdoRs. The new ligands were designed to better explore the receptor space around position 4 of the piperidine ring placing one or two substituents at C4. It should be emphasized that the spatial domain explored by 4-aryl substituents in piperidine and in piperazine derivatives does not overlap because aryl groups are linked to atoms with different geometry (i.e., a tetrahedral carbon [C4] and an almost planar nitrogen atom [N4]).

Considering the higher selectivity observed for 1-propyl-3-methylpiperazinamides compared to similarly substituted 1,3-diM and 1,3-diP congeners, most of the structural modifications at C4 were carried out on 1-propyl-3-methyl derivatives.

Piperidinamide ligands with both good hA_{2B} affinity (pK_i from 7.51 to 8.54) and hA_{2A}/hA_{2B} SI were obtained (Table 2). The plot of pK_i/hA_{2B} versus pK_i/hA_{2A} (Fig. 3) demonstrated that no correlation exists between the two sets of pK_i s and that a large number of ligands displayed elevated SIs. Unfortunately, it was not possible to determine the SI of 4,4-diphenyl derivatives **69** and **72** because their poor solubility in the assay medium prevented the measure of pK_i at hA_{2A} . Nonetheless, their very low percentage of radioligand displacements at 1 μ M allowed a safe rank of measured and roughly estimated hA_{2B}/hA_{2A} SIs. The SI of 1-propyl-3-methyl-diphenylpiperidinamide **69** proved significantly greater

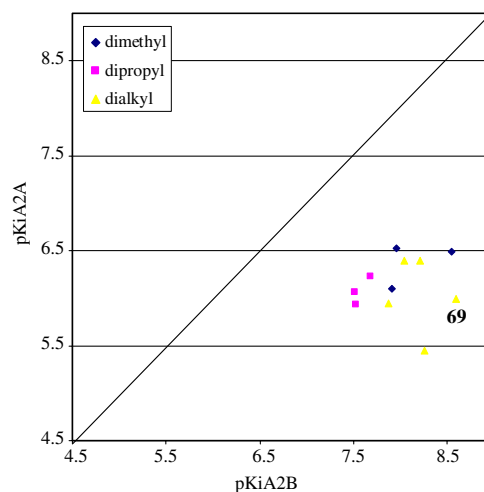


Figure 3. Affinity-selectivity plot for 1,3-dipropyl-9-dAX piperidinamides **67–81** (see Table 2).

than the corresponding diM (**72**) and diP (**77**) congeners; a similar ranking was observed for the 4-phenyl piperazinamide leads (i.e., **67** > **74** > **76**). These findings were consistent with the higher SIs observed for the 1-propyl, 3-methyl derivatives in the piperazine series. The introduction of an *ortho*-methoxy group on the 8-phenyl ring of **67** yielded a dramatic decrease, greater than two orders of magnitude, of hA_{2B} affinity in compound **79** as already seen for compound **36** in the piperazine series. The same explanation proposed for compound **36** (i.e., a conformational change leading to unfavourable steric interactions at position 4 of the piperidine/piperazine ring) may be advocated for ligand **79**.

Of particular interest were compounds **67** and **69** which showed outstanding hA_{2B} affinities ($K_i = 2.5$ and 5.5 nM, respectively) and selectivities (hA_{2A}/hA_{2B} SI = 398 and 630, respectively). Binding affinities of compound **69** were measured also at hA_1 and hA_3 AdoRs resulting in a pK_i of 6.17 for the former and 4% radioligand displacement at 1 μ M for the latter. These values indicated a good hA_1/hA_{2B} SI (120) and, presumably, also a much higher hA_3/hA_{2B} SI.

4.3. 1,3-Dialkyl-8-[4-phenoxy(*N*-1,2,3,4-tetrahydroisoquinoline)acetamido]-9-deazaxanthines

A small series of 9-dAX derivatives bearing tetrahydroisoquinoline as the NR^5R^6 moiety (structure **I**, Chart 2) and new R^1 and R^3 alkyl (or functionalized alkyl) substituents were prepared and evaluated for their affinity at hA_{2B} and hA_{2A} AdoRs. Ligands with good hA_{2B} affinity (pK_i 6.77–8.64) and hA_{2A}/hA_{2B} selectivity indexes were obtained (Table 3). The plot of pK_i/hA_{2B} versus pK_i/hA_{2A} in Figure 4 showed again no correlation between the two sets of pK_i s and allowed clear identification of a number of ligands with high SIs.

Among lead compounds **82**, **84** and **85**, 3-methyl,1-propyl derivative **84** displayed the highest hA_{2A}/hA_{2B} selectivity ratio (SI = 138) in accordance with previous data

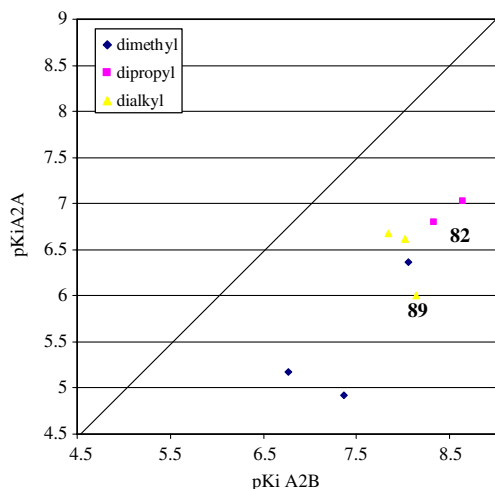


Figure 4. Affinity-selectivity plot for 1,3-dipropyl-9-dAX tetrahydroisoquinolinamides **82–90** (see Table 3).

from piperazin- and piperidinamide series. Another highly hA_{2B} selective compound was obtained by introducing an *ortho*-methoxy group on the 8-phenyl ring of lead compound **85**. Indeed, in ligand **89** the hA_{2A}/hA_{2B} SI jumped from 49 to 275 as a consequence of a decrease in hA_{2A} affinity that was significantly greater than in hA_{2B} (from 6.37 to 4.92 vs 8.06 to 7.36, respectively). In all probability, the conformational change induced by the introduction of methoxy group may place the tetrahydroisoquinoline ring, or preferably the fused benzo moiety, of **89** in an accessible region of the hA_{2B} -binding site analogously to what has been observed for the phenyl ring of anilide. $^{35}NR^5R^6$ moieties with a different topology, such as N4-/C4-phenyl piperazines/piperidines, in compounds **29** and **79**, respectively, might impact inaccessible regions of the hA_{2B} binding site resulting in a very low binding affinity. Plausible favoured and disfavoured binding topologies for the NR^5R^6 moieties of 8-*ortho*-methoxyphenyl derivatives are represented in a very schematic way in Figure 5, where accessible and inaccessible molecular fragments are coloured in green and red, respectively.

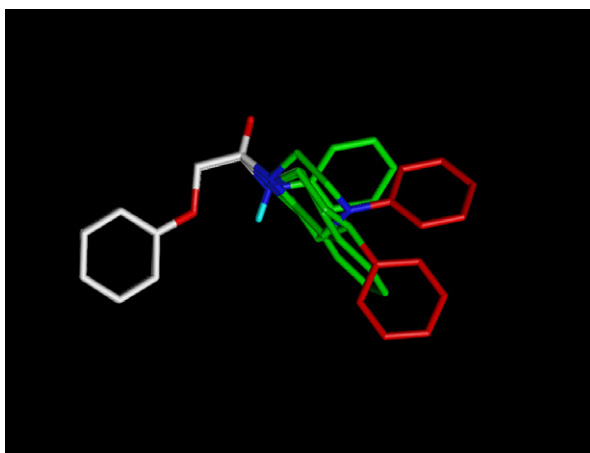


Figure 5. Molecular overlap of the 8-substituents in compounds **29**, **79** and **89**.

In expectation of the results of an ongoing 3D QSAR study on the entire array of data reported herein and in a previous account of our work.³⁵ Figure 5 may assist in interpreting the SAFIR and SSR of 8-*ortho*-methoxyphenyl-9-dAX derivatives.

4.4. Antagonist activity and efficacy of selected 9-dAX AdoR ligands at hA_{2A} and hA_{2B} AdoR subtypes

A number of ligands (i.e., **17**, **47**, **62**, **69** and **85**) were selected to measure their antagonistic potency through functional assays on isolated organs at cloned hA_{2B} and hA_{2A} AdoR subtypes. A representative example of this experiment is shown for compound **17** in Figure 1b. The pA_2 values at both receptor subtypes are reported in Table 4 along with the corresponding pK_i values from binding assays. pA_2 values very close to the corresponding pK_i s were obtained. Taken together, our findings indicate that binding affinity parallels antagonist potency and therefore binding and functional processes can be considered strictly related.

5. Conclusions

Careful design, synthesis and biological evaluation of a large series of novel 9-dAXs at the AdoR subtypes enabled the identification of an elevated number of ligands with outstanding hA_{2B} affinity ($pK_i > 8$) and a good hA_{2A}/hA_{2B} SI (>100). Among the compounds tested at the four AdoR subtypes, piperazine derivatives **23** and **52** as well as the piperidine derivative **69** resulted particularly interesting in terms of both high hA_{2B} affinity ($K_i = 11$, 2 and 5.5 nM, respectively) and selectivity towards hA_{2A} (SI $hA_{2A}/hA_{2B} = 912$, 159 and 630, respectively), hA_3 (hA_3/hA_{2B} SI >100 , 3090 and >180) and hA_1 (hA_1/hA_{2B} SI >100 , 44 and 120, respectively). Remarkably, in the present work the hA_1/hA_{2B} SI of some 9-dAXs was significantly improved compared to the anilide derivatives (Chart 2, structure **I**, $NR^5R^6 = NHAr$) reported in our previous paper.³⁵

A number of selected ligands (Table 4), tested in functional assays *in vitro*, showed very interesting antagonist activities and efficacies at both A_{2A} and A_{2B} AdoR subtypes, consistent with their affinities measured in the binding assays.

The present study allowed us to identify the key molecular determinants of high hA_{2B} affinity and, more importantly, high hA_{2B} selectivity. The most salient features emerging from the SSR and SAFIR can be summarized as follows: (i) 1-propyl-3-methyl substitution significantly increased the hA_{2A}/hA_{2B} SIs compared to 1,3-diM and 1,3-diP analogues; (ii) the introduction of an *ortho*-methoxy substituent in the 8-phenyl ring afforded highly hA_{2B} selective ligands but strictly depending upon the nature, size and topology of the NR^5R^6 substituents; (iii) lipophilic substituents at the N4 position of piperazinamides as well as lipophilic groups at the *meta* and *para* positions of the N4-phenyl ring significantly augmented hA_{2B} affinity; and (iv) the introduction of one or two methyl groups on the oxyacetamido

bridge led to a diminution of hA_{2B} affinity in both the diM and diP series, the gem-dimethyl derivatives being generally less active than the corresponding mono-methyl congeners.

The effect on the hA_{2B} affinity of the substitution pattern at positions 1 and 3 was less clear than that emerging from hA_{2B} selectivity. In fact, the ranking of hA_{2B} affinity of N4-phenyl leads differed for the piperazinamides and the tetrahydroisoquinolinamides (the two most explored series) according to the following decreasing order of affinity, respectively:

1,3-Dipropyl (**40**) \approx 1,3-di-2-methoxyethyl (**55**) \approx 1,3-dimethyl (**17**) > 1-isobutyl-3-methyl (**58**) > 1,3-dicyclopropyl (**59**) \approx 1-methyl,3-propyl (**60**) > 1,3-diethyl (**63**) \approx 1-propyl,3-methyl (**64**) > 1,3-ditrifluoroethyl (**66**) and 1,3-dipropyl (**82**) > 1-propyl,3-methyl (**84**) \approx 1,3-dimethyl (**85**) \approx 1,3-dicyclopropyl (**86**) > 1-methyl,3-propyl (**87**) \approx 1,3-di-2-methoxyethyl (**88**).

However, it is important to note that in both the series the most and less active ligands carry the same substituents at 1,3 positions.

In conclusion, taken together, the data reported in our previous³⁵ and in this companion paper confirmed that suitably substituted 9-dAXs represent highly potent and hA_{2B} selective antagonists that may hold great promise as antiasthmatic agents. Further studies will be performed to assess off-target activities of our compounds (e.g., HERK and CYP inhibition) and to confirm their efficacy as antiasthmatic agents through in vitro and in vivo assays, such as degranulation of human isolated mastocytes³⁶ and tests on animal models such as actively sensitized Brown Norway rats.³⁷

6. Experimental

High analytical grade chemicals and solvents were from commercial suppliers. When necessary, solvents were dried by standard techniques and distilled. After extraction from aqueous phases, the organic solvents were dried over anhydrous magnesium or sodium sulfate. Thin-layer chromatography (TLC) was performed on aluminium sheets precoated with silica gel 60 F254 (0.2 mm) type E. Merck. Chromatographic spots were visualized by UV light or Hanessian reagent.³⁸

Purification of crude compounds was carried out by flash column chromatography on silica gel 60 (Kieselgel 0.040–0.063 mm, E. Merck) or by crystallization. Melting points (uncorrected) for fully purified products (see below) were determined in a glass capillary tube on a Stuart Scientific electrothermal apparatus SMP3. ¹H NMR spectra were recorded on a 300 MHz Bruker AMX-300 spectrometer. All the detected signals were in accordance with the proposed structures. Chemical shifts (δ scale) are reported in parts per million (ppm) relative to the central peak of the solvent. Coupling constant (J values) are given in hertz (Hz). Spin multiplicities are given as: s (singlet), d (doublet), dd (doublet), t (triplet), or m (multiplet), br s (broad singlet), dt (double triplet). Electron impact mass (EI-MS) or electron spray ionization mass (ESI-MS) were recorded in a quadrupolar Hewlett-Packard 5988 and in Waters ZQ 4000 apparatus, respectively. Elemental analyses were performed on a Eurovector 300 C, H, N analyzer. Fully purified products had satisfactory C, H, N analyses (within $\pm 0.4\%$ of theoretical values). Non-high-throughput chemical reactions were generally carried out under an argon atmosphere whereas dry nitrogen was used in parallel syntheses. Parallel reactions were performed on a Chemspeed ASW 1000 instrument. In several instances, the final products obtained by parallel synthesis were rapidly purified by flash column chromatography up to an acceptable purity (better than 90–95% by HPLC check) and tested without further purification. In such a case only ESI/MS or EI/MS spectra and HPLC retention times were listed (see [Supplementary Material](#)). The HPLC analyses were performed on a Symmetry C18 (2.1 \times 10 mm) column on a Waters 2690 instrument. As detectors, Micromass ZMD for ES ionization or Waters 996 Diode Array were used. Diode array chromatograms were processed at 210 nm. The mobile phases were a mixture of formic acid (0.46 mL), aqueous ammonia 33% (0.115 mL) and water (1000 mL) (phase A) and a quaternary mixture of formic acid (0.4 mL), ammonia (0.1 mL), methanol (500 mL), and acetonitrile (500 mL) (phase B). A gradient technique was applied going from A 100% to 95% B in 20 min. The flow rate was 0.4 mL/min. The injection volume was 5 μ L.

For compounds prepared by conventional organic synthesis (i.e., **17**, **22**, **24**, **25**, **30**, **31**, **33**, **35**, **36**, **40**, **41**, **67**, **73**, **74**, **76**, **79**, **82** and **85**) besides the spectral data (i.e., ¹H NMR, ESI/MS or EI/MS spectra) also melting points and microanalyses were determined. The syntheses of oxyacetic acids **II** and oxyacetic esters **III** of 9-deazaxanthine derivatives have been already described.³⁵

For compounds prepared by conventional organic synthesis (i.e., **17**, **22**, **24**, **25**, **30**, **31**, **33**, **35**, **36**, **40**, **41**, **67**, **73**, **74**, **76**, **79**, **82** and **85**) besides the spectral data (i.e., ¹H NMR, ESI/MS or EI/MS spectra) also melting points and microanalyses were determined. The syntheses of oxyacetic acids **II** and oxyacetic esters **III** of 9-deazaxanthine derivatives have been already described.³⁵

6.1. General procedures for the amidation of oxyacetic acids and oxyacetic esters of 9-deazaxanthine derivatives (see [Scheme 1](#))

The synthesis of the target amides was performed by using one of the following methods (A–D).

6.1.1. Method A. The reaction took place in a sealed tube under argon atmosphere. To 0.15 mmol of the ester **III** (see [Scheme 1](#)) and 16.00 mmol of amines was added a catalytic amount of sodium cyanide (5 mg). In the case of liquid amines the reaction mixture was heated at the boiling temperature of the amine whereas for solid amines 2 mL of anhydrous dioxane was used as solvent and the reaction mixture heated at 100 °C. The reactions were monitored by TLC, and when no more starting material was observed, the mixture was cooled to room temperature and the final product isolated by filtration and washed with ethyl ether and crystallized from H₂O/MeOH. When no precipitate was formed, the reaction mixture was concentrated under reduced pressure and the residue purified by flash column chromatography on silica gel.

6.1.2. Method B. A solution of the proper carboxylic acid (**II**, see Scheme 1) (0.72 mmol) in anhydrous tetrahydrofuran (20 mL) under argon atmosphere was cooled to -40°C , and *N*-methylmorpholine (0.08 mL, 0.72 mmol) and isobutyl chloroformate (0.09 mL, 0.72 mmol) were slowly added. The mixture was stirred at -40°C for 2 h. Then the appropriate amine (0.72 mmol) was added, and the mixture was stirred 15 min at -40°C and then for additional 12 h at room temperature. The solution was evaporated under reduced pressure, and the residue was dissolved in DCM, washed with a saturated solution of sodium bicarbonate, water and brine, and then dried (Na_2SO_4) and evaporated under reduced pressure. The resulting crude product was purified by flash column chromatography on silica gel or crystallized by $\text{H}_2\text{O}/\text{MeOH}$.

6.1.3. Method C. To a mixture of the carboxylic acid (**II**, see Scheme 1) (1.24 mmol), *N*-(3-dimethylaminopropyl)-*N'*-ethylcarbodiimide hydrochloride (0.28 g, 1.49 mmol), 1-hydroxybenzotriazole (0.20 g, 1.49 mmol), triethylamine (0.35 mL, 2.48 mmol) and anhydrous DCM (20 mL) was added the appropriate amine (1.61 mmol) and the mixture was stirred at room temperature overnight under argon atmosphere. The resulting solution was evaporated under reduced pressure, and the residue was dissolved in DCM and washed with a saturated sodium bicarbonate aqueous solution. The organic phase was separated, washed with water and brine, dried (Na_2SO_4) and evaporated under reduced pressure. The resulting crude was purified by flash column chromatography on silica gel or crystallized by $\text{H}_2\text{O}/\text{MeOH}$.

6.1.4. Method D. To a mixture of the carboxylic acid (**II**, see Scheme 1) (0.21 mmol), *N*-(3-dimethylaminopropyl)-*N'*-ethylcarbodiimide hydrochloride (0.09 g, 0.23 mmol), 1-hydroxybenzotriazole (0.30 g, 0.23 mmol) and polymer bound morpholine (0.28 g, 2.75 mmol/g based on nitrogen analysis) in anhydrous DMF (4 mL) was added the suitable amine (0.23 mmol), and the mixture was stirred overnight at room temperature. To the resulting solution were added macroporous triethylammonium methylpolystyrene carbonate (0.25 g, 2.8–3.5 mmol/g based on nitrogen elemental analysis) and Amberlyst 15 (0.65 g) as scavengers, and the suspension was stirred for 2 h (in the case of acidic or basic final products the corresponding scavenger was not added). The resulting suspension was filtered and evaporated under reduced pressure. The residue was triturated with a mixture of $\text{MeOH}/\text{ethyl ether}$, and the precipitate was collected by filtration to yield the desired product in a sufficient purity for biological testing.

6.1.4.1. 1,3-Dimethyl-6-{4-[2-oxo-2-(4-phenylpiperazin-1-yl)ethoxy]phenyl}-1*H*-pyrrolo[3,2-*d*]pyrimidine-2,4(3*H*,5*H*)-dione (17). Method A, Yield 25%, mp: $>250^{\circ}\text{C}$, $^1\text{H NMR}$ (CDCl_3): 11.25 (s, 1H), 7.76 (d, $J = 8.7$ Hz, 2H), 7.29–7.27 (m, 3H), 7.02 (d, $J = 8.7$ Hz, 2H), 6.92–6.90 (m, 2H), 6.18 (s, 1H), 4.80 (s, 2H), 3.80–3.76 (m, 4H), 3.53 (s, 3H), 3.49 (s, 3H), 3.49–3.45 (m, 4H). MS (EI) m/z : 473 $[\text{M}]^+$ Anal. Calcd for $\text{C}_{26}\text{H}_{27}\text{N}_5\text{O}_4$: C, 65.93; H, 5.75; N, 14.79. Found: C, 66.23; H, 5.96; N, 15.01.

6.1.4.2. 6-(4-{2-[4-(4-Fluorophenyl)piperazin-1-yl]-2-oxoethoxy}phenyl)-1,3-dimethyl-1*H*-pyrrolo[3,2-*d*]pyrimidine-2,4(3*H*,5*H*)-dione (22). Method A, Yield 50%, mp: $>250^{\circ}\text{C}$, $^1\text{H NMR}$ ($\text{DMSO}-d_6$): 12.30 (br s, 1H), 7.84 (d, $J = 8.5$ Hz, 2H), 7.06–7.02 (m, 6H), 6.63 (s, 1H), 4.95 (s, 2H), 3.64–3.60 (m, 4H), 3.42 (s, 3H), 3.26 (s, 3H), 3.14–3.10 (m, 2H), 3.09–3.05 (m, 2H). MS (EI) m/z : 491 $[\text{M}]^+$, Anal. Calcd for $\text{C}_{26}\text{H}_{26}\text{FN}_5\text{O}_4$: C, 63.53; H, 5.33; N, 14.25. Found: C, 63.71; H, 5.54; N, 14.51.

6.1.4.3. 6-(4-{2-[4-(4-Methoxyphenyl)piperazin-1-yl]-2-oxoethoxy}phenyl)-1,3-dimethyl-1*H*-pyrrolo[3,2-*d*]pyrimidine-2,4(3*H*,5*H*)-dione (24). Method A, Yield 28%, mp: $>250^{\circ}\text{C}$, $^1\text{H NMR}$ ($\text{DMSO}-d_6$): 12.38 (br s, 1H), 7.96 (d, $J = 8.8$ Hz, 2H), 7.09 (d, $J = 9.3$ Hz, 2H), 7.05 (d, $J = 8.8$ Hz, 2H), 6.96 (d, $J = 9.3$ Hz, 2H), 6.74 (s, 1H), 5.06 (s, 2H), 3.81 (s, 3H), 3.75–3.71 (m, 4H), 3.54 (s, 3H), 3.38 (s, 3H), 3.21–3.17 (m, 2H), 3.13–3.09 (m, 2H), MS (EI) m/z : 503 $[\text{M}]^+$ Anal. Calcd for $\text{C}_{27}\text{H}_{29}\text{N}_5\text{O}_5$: C, 64.40; H, 5.80; N, 13.91. Found: C, 64.66; H, 5.83; N, 14.06.

6.1.4.4. 1,3-Dimethyl-6-{4-[2-oxo-2-(4-pyrimidin-2-yl)piperazin-1-yl]ethoxy]phenyl}-1*H*-pyrrolo[3,2-*d*]pyrimidine-2,4(3*H*,5*H*)-dione (25). Method A, Yield 60%, mp: $>250^{\circ}\text{C}$, $^1\text{H NMR}$ ($\text{DMSO}-d_6$): 12.27 (br s, 1H), 8.41 (d, $J = 4.7$ Hz, 2H), 7.85 (d, $J = 8.8$ Hz, 2H), 7.03 (d, $J = 8.8$ Hz, 2H), 6.69 (t, $J = 4.7$ Hz, 1H), 6.63 (s, 1H), 4.96 (s, 2H), 3.85–3.81 (m, 2H), 3.78–3.76 (m, 2H), 3.59–3.55 (m, 4H), 3.43 (s, 3H), 3.27 (s, 3H). MS (EI) m/z : 475 $[\text{M}]^+$, Anal. Calcd for $\text{C}_{24}\text{H}_{25}\text{N}_7\text{O}_4$: C, 60.62; H, 5.30; N, 20.60. Found: C, 60.82; H, 5.45; N, 20.78.

6.1.4.5. 6-(4-{2-[4-(2-Methoxyphenyl)piperazin-1-yl]-2-oxoethoxy}phenyl)-1,3-dimethyl-1*H*-pyrrolo[3,2-*d*]pyrimidine-2,4(3*H*,5*H*)-dione (30). Method A, Yield 60%, mp: 181–183 $^{\circ}\text{C}$, $^1\text{H NMR}$ ($\text{DMSO}-d_6$): 12.21 (br s, 1H), 7.78–7.74 (m, 2H), 6.88–6.84 (m, 6H), 6.52 (s, 1H), 4.88 (s, 2H), 3.76 (s, 3H), 3.60–3.56 (m, 4H), 3.38 (s, 3H), 3.22 (s, 3H), 2.51–2.47 (m, 4H). MS (EI) m/z : 503 $[\text{M}]^+$, Anal. Calcd for $\text{C}_{27}\text{H}_{29}\text{N}_5\text{O}_5$: C, 64.40; H, 5.80; N, 13.91. Found: C, 64.56; H, 5.91; N, 14.22.

6.1.4.6. 6-{4-[2-(4-Benzylpiperazin-1-yl)-2-oxoethoxy]phenyl}-1,3-dimethyl-1*H*-pyrrolo[3,2-*d*]pyrimidine-2,4(3*H*,5*H*)-dione (31). Method A, Yield 40%, mp: 170–172 $^{\circ}\text{C}$, $^1\text{H NMR}$ ($\text{DMSO}-d_6$): 12.05 (br s, 1H), 7.64 (d, $J = 8.2$ Hz, 2H), 7.14 (s, 5H), 6.78 (d, $J = 8.2$ Hz, 2H), 6.38 (s, 1H), 4.68 (s, 2H), 3.23–3.17 (m, 6H), 2.26–2.22 (m, 2H), 2.20–2.14 (m, 2H). EI/MS 487 m/z $[\text{M}]^+$, Anal. Calcd for $\text{C}_{27}\text{H}_{29}\text{N}_5\text{O}_4$: C, 66.51; H, 6.01; N, 14.36. Found: C, 66.82; H, 6.11; N, 14.65.

6.1.4.7. 1,3-Dimethyl-6-{4-[2-oxo-2-(4-pyridin-2-yl)piperazin-1-yl]ethoxy]phenyl}-1*H*-pyrrolo[3,2-*d*]pyrimidine-2,4(3*H*,5*H*)-dione (33). Method A, Yield 42%, mp: $>250^{\circ}\text{C}$, $^1\text{H NMR}$ ($\text{DMSO}-d_6$): 12.15 (br s, 1H), 8.14 (d, $J = 4.5$ Hz, 1H), 7.84 (d, $J = 7.9$ Hz, 2H), 7.59–7.55 (m, 1H), 7.01 (d, $J = 7.9$ Hz, 2H), 6.90–6.86 (m, 1H), 6.70–6.66 (m, 1H), 6.60 (s, 1H), 4.91 (s, 2H), 3.60–3.26 (m, 14H). MS (EI) m/z : 474 $[\text{M}]^+$, Anal. Calcd for $\text{C}_{25}\text{H}_{26}\text{N}_6\text{O}_4$: C, 63.28; H, 5.52; N, 17.71. Found: C, 63.31; H, 5.61; N, 17.88.

6.1.4.8. 1,3-Dimethyl-6-{4-[2-(4-methylpiperazin-1-yl)-2-oxoethoxy]phenyl}-1H-pyrrolo[3,2-d]pyrimidine-2,4(3H,5H)-dione (35). Method C, Yield 72%, mp: >250 °C, ¹H NMR (DMSO-*d*₆): 12.09 (br s, 1H), 7.84 (d, *J* = 8.7 Hz, 2H), 6.97 (d, *J* = 8.7 Hz, 2H), 6.57 (s, 1H), 4.88 (s, 2H), 3.42 (s, 3H), 3.27 (s, 3H), 2.53–2.49 (m, 2H), 2.37–2.33 (m, 2H), 2.29–2.25 (m, 2H), 2.15–2.11 (m, 2H). MS (EI) *m/z*: 411 [M]⁺, Anal. Calcd for C₂₁H₂₅N₅O₄: C, 61.30; H, 6.12; N, 17.02. Found: C, 61.43; H, 6.34; N, 17.14.

6.1.4.9. 6-(4-{2-[4-(4-Chlorophenyl)piperazin-1-yl]-2-oxoethoxy}-2-methoxyphenyl)-1,3-dimethyl-1H-pyrrolo[3,2-d]pyrimidine-2,4(3H,5H)-dione (36). Method A, Yield 72%, mp: 191–193 °C, ¹H NMR (DMSO-*d*₆): 11.78 (s, 1H), 7.69 (d, *J* = 8.5 Hz, 1H), 7.24 (d, *J* = 8.8 Hz, 2H), 6.97 (d, *J* = 8.8 Hz, 2H), 6.69 (m, 1H) 6.61–6.57 (m, 1H) 6.51 (s, 1H), 4.93 (s, 2H), 3.86 (s, 3H), 3.62–3.58 (m, 4H), 3.39 (s, 3H), 3.23 (s, 3H), 3.22–3.14 (m, 4H). MS (EI) *m/z*: EI/MS 537 [M]⁺, Anal. Calcd for C₂₇H₂₈ClN₅O₅: C, 60.28; H, 5.25; N, 13.02. Found: C, 59.89; H, 5.35; N, 13.30.

6.1.4.10. 6-{4-[2-Oxo-2-(4-phenylpiperazin-1-yl)ethoxy]phenyl}-1,3-dipropyl-1H-pyrrolo[3,2-d]pyrimidine-2,4(3H,5H)-dione (40). Method B, Yield 29%, mp: 181–183 °C, ¹H NMR (DMSO-*d*₆): 12.15 (s, 1H), 7.86 (d, *J* = 8.8 Hz, 2H), 7.27–7.23 (m, 2H), 7.02–6.98 (m, 4H), 6.85–6.81 (m, 1H), 6.66 (s, 1H), 4.96 (s, 2H), 3.89–3.85 (m, 4H), 3.65–3.61 (m, 4H), 3.23–3.19 (m, 2H), 3.16–3.12 (m, 2H), 2.54–2.49 (m, 4H), 1.10–0.80 (m, 6H). MS (EI) *m/z*: 529 [M]⁺, Anal. Calcd for C₃₀H₃₅N₅O₄: C, 68.03; H, 6.66; N, 13.22. Found: C, 68.44; H, 6.97; N, 13.43.

6.1.4.11. 6-{4-[2-(4-Benzylpiperazin-1-yl)-2-oxoethoxy]phenyl}-1,3-dipropyl-1H-pyrrolo[3,2-d]pyrimidine-2,4(3H,5H)-dione (41). Method C, Yield 35%, mp: >250 °C, ¹H NMR (DMSO-*d*₆): 12.20 (s, 1H), 7.81 (d, *J* = 8.5 Hz, 2H), 7.34 (s, 5H), 6.95 (d, *J* = 8.5 Hz, 2H), 6.63 (s, 1H), 4.85 (s, 2H), 3.86–3.81 (m, 4H), 3.47 (s, 2H), 3.46–3.43 (m, 4H), 2.39–2.24 (m, 4H), 1.69–1.51 (m, 4H), 0.91–0.81 (m, 6H). MS (EI) *m/z*: 534 [M]⁺, Anal. Calcd for C₃₁H₃₇N₅O₄: C, 68.49; H, 6.86; N, 12.88. Found: C, 68.15; H, 6.53; N, 12.53.

6.1.4.12. 1-Methyl-6-{4-[2-oxo-2-(4-phenylpiperidin-1-yl)ethoxy]phenyl}-3-propyl-1H-pyrrolo[3,2-d]pyrimidine-2,4(3H,5H)-dione (67). Method C, Yield 54%, mp: 225–227 °C, ¹H NMR (DMSO-*d*₆): 12.23 (s, 1H), 7.82 (d, *J* = 8.8 Hz, 2H), 7.30–7.50 (m, 5H), 6.99 (d, *J* = 8.8 Hz, 2H), 6.59 (s, 1H), 4.90 (s, 2H), 4.48–4.44 (m, 1H), 3.97–3.92 (m, 1H), 3.84 (t, *J* = 7.2 Hz, 2H), 3.79 (s, 3H), 3.17–3.09 (m, 1H), 2.86–2.54 (m, 3H), 1.93–1.80 (m, 2H), 1.70–1.42 (m, 2H), 0.85 (t, *J* = 7.3 Hz, 3H). MS (EI) *m/z*: 501 [M+H]⁺, Anal. Calcd for C₂₈H₃₁N₅O₄: C, 67.05; H, 6.23; N, 13.96. Found: C, 67.23; H, 6.32; N, 13.80.

6.1.4.13. 6-(4-{2-[4-(4-Fluorobenzoyl)piperidin-1-yl]-2-oxoethoxy}phenyl)-1,3-dimethyl-1H-pyrrolo[3,2-d]pyrimidine-2,4(3H,5H)-dione (73). Method C, Yield 40%, mp: >250 °C, ¹H NMR (DMSO-*d*₆): 12.29 (s, 1H), 8.13 (dd,

J = 8.5, 5.7 Hz, 2H), 7.85 (d, *J* = 8.6 Hz, 2H), 7.40–7.36 (m, 2H), 7.00 (d, *J* = 8.6 Hz, 2H), 6.65 (s, 1H), 4.92 (s, 2H), 4.37 (m, 1H), 3.92 (m, 1H), 3.76 (m, 1H), 3.47 (m, 1H), 3.43 (s, 3H), 3.27 (s, 3H), 2.82 (m, 1H), 1.84 (m, 2H), 1.61 (m, 1H), 1.41 (m, 1H). MS (EI) *m/z*: 518 [M]⁺, Anal. Calcd for C₂₈H₂₇N₄O₅: C, 64.86; H, 5.25; N, 10.80. Found: C, 64.73; H, 4.98; N, 10.43.

6.1.4.14. 1,3-Dimethyl-6-{4-[2-oxo-2-(4-phenylpiperidin-1-yl)ethoxy]phenyl}-1H-pyrrolo[3,2-d]pyrimidine-2,4(3H,5H)-dione (74). Method B, Yield 52%, mp: >250 °C, DMSO-*d*₆: 12.23 (s, 1H), 7.83 (d, *J* = 8.9 Hz, 2H), 7.31–7.16 (m, 5H), 6.99 (d, *J* = 8.9 Hz, 2H), 6.56 (s, 1H), 4.90 (s, 2H), 4.49–4.45 (m, 1H), 3.97–3.93 (m, 1H), 3.40 (s, 3H), 3.24 (s, 3H), 3.17–3.09 (m, 1H) 2.87–2.72 (m, 2H), 1.85–1.76 (m, 2H), 1.67–1.63 (m, 1H), 1.46–1.42 (m, 1H). MS (EI) *m/z*: 472 [M]⁺, Anal. Calcd for C₂₇H₂₈N₄O₄: C, 68.63; H, 5.97; N, 11.86. Found: C, 68.41; H, 5.75; N, 11.65.

6.1.4.15. 6-{4-[2-Oxo-2-(4-phenylpiperidin-1-yl)ethoxy]phenyl}-1,3-dipropyl-1H-pyrrolo[3,2-d]pyrimidine-2,4(3H,5H)-dione (76). Method B, Yield 48%, mp: >250 °C, ¹H NMR (CDCl₃): 10.49 (s, 1H), 7.96–7.61 (m, 2H), 7.32–7.14 (m, 5H), 7.06 (d, *J* = 8.6 Hz, 2H), 6.18 (s, 1H), 4.79 (s, 2H), 4.29–4.27 (m, 1H), 4.14–4.13 (m, 1H), 4.08–3.91 (m, 4H), 3.21–3.17 (m, 1H) 2.72–2.71 (m, 2H), 2.17–1.68 (m, 10H), 1.03–0.91 (m, 6H). MS (EI) *m/z*: 528 [M]⁺, Anal. Calcd for C₃₁H₃₆N₄O₄: C, 70.43; H, 6.86; N, 10.60. Found: C, 70.23; H, 6.67; N, 10.40.

6.1.4.16. 6-{2-Methoxy-4-[2-oxo-2-(4-phenylpiperidin-1-yl)ethoxy]phenyl}-1,3-dimethyl-1H-pyrrolo[3,2-d]pyrimidine-2,4(3H,5H)-dione (79). Method C, Yield 53%, mp: 230–232 °C, ¹H NMR (DMSO-*d*₆): 11.79 (s, 1H), 7.70 (d, *J* = 8.8 Hz, 1H), 7.31–7.15 (m, 5H), 6.69–6.65 (m, 1H), 6.59–6.54 (m, 1H), 6.51 (s, 1H), 4.90 (s, 2H), 4.50–4.45 (m, 1H), 4.00–3.95 (m, 1H), 3.86 (s, 3H), 3.41 (s, 3H), 3.24 (s, 3H), 3.19–3.10 (m, 1H), 2.87–2.52 (m, 1H), 1.88–1.78 (m, 2H), 1.70–1.63 (m, 1H), 1.45–1.43 (m, 1H). MS (EI) *m/z*: 502 [M]⁺, Anal. Calcd for C₂₈H₃₀N₄O₅: C, 66.92; H, 6.02; N, 11.15. Found: C, 67.01; H, 6.24; N, 11.36.

6.1.4.17. 6-{4-[2-(3,4-Dihydroisoquinolin-2(1H)-yl)-2-oxoethoxy]phenyl}-1,3-dipropyl-1H-pyrrolo[3,2-d]pyrimidine-2,4(3H,5H)-dione (82). Method B, Yield 30%, mp: 174–176 °C, ¹H NMR (DMSO-*d*₆): 12.01 (s, 1H), 7.62 (d, *J* = 8.7 Hz, 2H), 6.98 (s, 4H), 6.79 (d, *J* = 8.7 Hz, 2H), 6.43 (s, 1H), 4.77 (s, 2H), 3.60–3.54 (m, 4H), 3.26–3.22 (m, 2H), 2.67–2.60 (m, 2H), 2.31–2.27 (m, 2H), 1.46–1.37 (m, 4H), 1.10–0.80 (m, 6H). MS (EI) *m/z*: 500 [M]⁺, Anal. Calcd for C₂₉H₃₂N₄O₄: C, 69.58; H, 6.45; N, 11.20. Found: C, 69.89; H, 6.38; N, 11.32.

6.1.4.18. 6-{4-[2-(3,4-Dihydroisoquinolin-2(1H)-yl)-2-oxoethoxy]phenyl}-1,3-dimethyl-1H-pyrrolo[3,2-d]pyrimidine-2,4(3H,5H)-dione (85). Method B, Yield 32%, mp: >250 °C, ¹H NMR (DMSO-*d*₆): 12.14 (br s, 1H), 7.71 (d, *J* = 8.5 Hz, 2H), 7.07 (s, 4H), 6.89 (d, *J* = 8.5 Hz, 2H), 6.50 (s, 1H), 4.86 (s, 2H), 3.58–3.54 (m, 2H), 3.37–3.33 (m, 2H), 3.29 (s, 3H), 3.13 (s, 3H), 2.74–2.72

(m, 1H), 2.41–2.37 (m, 1H). MS (EI) m/z : 444.2 [M]⁺, Anal. Calcd for C₂₅H₂₄N₄O₄: C, 67.55; H, 5.44; N, 12.60. Found: C, 67.67; H, 5.33; N, 12.43.

6.2. Biochemistry and pharmacology

6.2.1. Radioligand binding assays. Radioligand binding competition assays were performed in vitro using A₁, A_{2A}, A_{2B} and A₃ human receptors expressed in transfected CHO (*hA*₁), HeLa (*hA*_{2A} and *hA*₃) and HEK-293 (*hA*_{2B}) cells as described in detail in the [Supplementary material](#).

6.2.2. cAMP assays. These assay were performed on *hA*_{2A} and *hA*_{2B} receptors transfected in CHO cells by using the method described by Salomon³⁹ reported in the [Supplementary material](#).

6.2.3. Isolated organ assays

6.2.3.1. A_{2A} receptors. These assays were performed on A_{2A} receptors⁴⁰ from isolated aorta of 200–250 g male Sprague–Dawley rats as reported in detail in the [Supplementary material](#).

6.2.3.2. A_{2B} receptors. These assays were performed on A_{2B} receptors⁴¹ from isolated aorta of 300–350 g male guinea pigs as reported in detail in the [Supplementary material](#).

Acknowledgment

The authors thanks the MIUR (Ministero dell'Università e della Ricerca Scientifica, Rome (Italy)), for partial financial support.

Supplementary data

ESI/MS or EI/MS spectra and HPLC retention times for compounds prepared by parallel synthesis, biological and pharmacological experimental data are reported. Supplementary data associated with this article can be found, in the online version, at [Supplementary data associated with this article can be found, in the online version, at doi:10.1016/j.bmc.2008.01.002](#).

References and notes

- Jacobson, K. A.; Gao, Z.-G. *Nat. Rev. Drug Discov.* **2006**, *5*, 247.
- Moro, S.; Gao, Z.-G.; Jacobson, K. A.; Spalluto, G. *Med. Res. Rev.* **2006**, *26*, 131.
- Akkari, R.; Burbiel, J. C.; Hockemeyer, J.; Müller, C. E. *Curr. Top. Med. Chem.* **2006**, *6*, 1375.
- Fredholm, B. B.; IJzerman, A. P.; Jacobson, K. A.; Klotz, K. N.; Linden, J. *Pharmacol. Rev.* **2001**, *53*, 527.
- Volpini, R.; Costanzi, S.; Vittori, S.; Cristalli, G.; Klotz, K.-N. *Curr. Top. Med. Chem.* **2003**, *3*, 427.
- Baraldi, P. G.; Romagnoli, R.; Preti, D.; Fruttarolo, F.; Carrion, M. D.; Tabrizi, M. A. *Curr. Med. Chem.* **2006**, *13*, 3467.
- Strohmeier, G. R.; Reppert, S. M.; Lencer, W. I.; Madara, J. L. *J. Biol. Chem.* **1995**, *270*, 2387.
- Papassotiropoulos, A.; Hock, C.; Nitsch, R. M. *Neurobiol. Aging* **2001**, *22*, 903.
- Harada, H.; Osamu Asano, O.; Hoshino, Y.; Yoshikawa, S.; Matsukura, M.; Kabasawa, Y.; Nijima, J.; Kotake, Y.; Watanabe, N.; Kawata, T.; Inoue, T.; Horizoe, T.; Yasuda, N.; Minami, H.; Nagata, K.; Murakami, M.; Nagaoka, J.; Kobayashi, S.; Tanaka, I.; Abe, S. *J. Med. Chem.* **2001**, *44*, 170.
- Linden, J. *Mol. Pharmacol.* **2005**, *67*, 1385.
- Jacobson, K. A.; Hoffman, C.; Cattabeni, F.; Abbracchio, M. P. *Apoptosis* **1999**, *4*, 197.
- Xaus, J.; Valledor, A. F.; Cardo, M.; Marques, L.; Beleta, J.; Palacios, J. M.; Celada, A. *J. Immunol.* **1999**, *163*, 4140.
- Fozard, J. R.; McCarthy, C. *Curr. Opin. Invest. Drugs* **2002**, *3*, 69.
- Feoktistov, I.; Biaggioni, I. *J. Clin. Invest.* **1995**, *96*, 1979.
- Wolber, C.; Fozard, J. R. *Naunyn Schmiedeberg's Arch. Pharmacol.* **2005**, *371*, 158.
- Holgate, S. T. *Br. J. Pharmacol.* **2005**, *145*, 1009.
- Feoktistov, I.; Murray, J. J.; Biaggioni, I. *Mol. Pharmacol.* **1994**, *45*, 1160.
- Peyrot, M.-L.; Gadeau, A.-P.; Dandré, F.; Belloc, I.; Dupuch, F.; Desgranges, C. *Circ. Res.* **2000**, *86*, 76.
- Robeva, A. S.; Woodward, R.; Jin, X.; Gao, Z.-J.; Bhattacharya, S.; Taylor, H. E.; Rosin, D. L.; Linden, J. *Drug Dev. Res.* **1996**, *39*, 243.
- Jacobson, K. A.; Ukena, D.; Padgett, W.; Daly, J. W.; Kirk, K. L. *J. Med. Chem.* **1987**, *30*, 211.
- Müller, C. E.; Shi, D.; Manning, M.; Daly, J. W. *J. Med. Chem.* **1993**, *36*, 3341.
- Carotti, A.; Stefanachi, A.; Ravina, E.; Sotelo, E.; Loza, M. I.; Cadavid, M. I.; Centeno, N. B.; Nicolotti, O. *Eur. J. Med. Chem.* **2004**, *39*, 879.
- Kim, S. A.; Marshall, M. A.; Melman, N.; Kim, H. S.; Müller, C. E.; Linden, J.; Jacobson, K. A. *J. Med. Chem.* **2002**, *45*, 2131.
- Grahner, B.; Winiwarter, S.; Lanzer, W.; Müller, C. E. *J. Med. Chem.* **1994**, *37*, 1526.
- Hayallah, A.; Sandoval-Ramirez, J.; Reith, U.; Schobert, U.; Preiss, B.; Schumacher, B.; Daly, J. W.; Müller, C. E. *J. Med. Chem.* **2002**, *45*, 1500.
- Vidal, B. J.; Esteve Trias, C.; Segarra Matamoros, V.; Ravina Rubira, E.; Fernandez Gonzales, F.; Loza Garcia, M. I.; Sanz Carreras, F. 6-WO Patent 03/000694, 2003.
- Kalla, R.; Perry, T.; Elzein, E.; Varkhedkar, V.; Li, X.; Ibrahim, P.; Palle, V.; Xiao, D.; Zablocki, J. US Patent 6825349, 2004.
- Palle, V.; Elzein, E.; Ibrahim, P.; Kalla, R.; Li X.; Perry T.; Varkhedkar, V.; Xiao, D.; Zablocki, J. WO Patent 05042534, 2005.
- Wang, G.; Rieger, J. M.; Thompson, R. D. WO Patent 05021548, 2005.
- Kim, Y. C.; Ji, X.; Melman, N.; Linden, J.; Jacobson, K. A. *Drug Dev. Res.* **1999**, *47*, 178.
- Kim, Y. C.; Ji, X.; Melman, N.; Linden, J.; Jacobson, K. A. *J. Med. Chem.* **2000**, *43*, 1165.
- Baraldi, P. G.; Tabrizi, M. A.; Preti, D.; Bovero, A.; Romagnoli, R.; Fruttarolo, F.; Abdel Zaid, N.; Moorman, A. R.; Varani, K.; Gessi, S.; Merighi, S.; Borea, P. A. *J. Med. Chem.* **2004**, *47*, 1434.
- Zablocki, J.; Kalla, R.; Perry, T.; Palle, V.; Varkhedkar, V.; Xiao, D.; Piscipio, A.; Maa, T.; Gimbel, A.; Hao, J.; Chu, N.; Leung, K.; Zeng, D. *Bioorg. Med. Chem. Lett.* **2005**, *15*, 609.
- Almirall Prodesfarma S. A.; Vidal, B.; Esteve, C. WO 03082873, 2003.
- Carotti, A.; Cadavid, M. I.; Centeno, N. B.; Esteve, C.; Loza, M. I.; Martinez, A.; Nieto, R.; Ravina, E.; Sanz, F.;

- Segarra, V.; Sotelo, E.; Stefanachi, A.; Vidal, B. *J. Med. Chem.* **2006**, *49*, 282.
36. Lago, J.; Alfonso, A.; Vieytes, M. R.; Botana, L. M. *Cell Signal.* **2001**, *13*, 515–524.
37. Hannon, J. P.; Tigani, B.; Williams, I.; Mazzoni, L.; Fozard, J. R. *Br. J. Pharmacol.* **2001**, *132*, 1509.
38. Touchstone, J. *Advances in Thin-Layer Chromatography*; Wiley: New York, 1982.
39. Salomon, Y. *Adv. Cyclic Nucleotide Res.* **1979**, *10*, 35.
40. Prentice, D. J.; Hourani, S. M. O. *Br. J. Pharmacol.* **1996**, *118*, 1509.
41. Alexander, S. P.; Losinsky, A.; Kendall, D. A.; Hill, S. J. A. *Br. J. Pharmacol.* **1994**, *111*, 185.